Hydrodynamic Dispersion and Mass Transfer in Unsaturated Flow

doi: 10.1029/1998WR900111

WATER RESOURCES RESEARCH, VOL. 35, NO. 4, PAGES 1065–1077, APRIL 1999

Hydrodynamic dispersion and mass transfer in unsaturated flow

D. Haga
Department of Geoscience and Technology, Graduate School of Engineering, Tohoku University, Sendai, Japan

Y. Niibori
Department of Quantum Science and Energy Engineering, Graduate School of Engineering, Tohoku University Sendai, Japan

T. Chida
Department of Geoscience and Technology, Graduate School of Engineering, Tohoku University, Sendai, Japan

Abstract. Tracer response experiments were carried out using a packed bed of glass beads, where fluid flowed as either a single phase (water) or two phases (water and gas) under steady unsaturated conditions. The results depended on the water saturation and could be divided into two regions at the critical water saturation, that is, the saturation at which the gas phase began to be immobile. To determine the hydrodynamic dispersion coefficients, the experimental responses were compared with the numerical results of a one-dimensional advection-dispersion equation. These results demonstrated that the hydrodynamic dispersion coefficients increased with a decrease in water saturation. Furthermore, the rates of the increase in the dispersion coefficients above the critical saturation were different from those below it. The following mathematical relations between the Peclet number, Pe, and the water saturation, S_w, were obtained from the results of the two unsaturated flow experiments: $Pe = 0.8S_w^{1.2}$ for single-phase flow and $Pe = 0.9S_w^{3.1}$ for two-phase flow. When $S_w = 1$ in the relation for single-phase flow, the value of Pe is in a range that has been reported previously. The relation for two-phase flow was used to analyze the mass transport of the two-phase tracer (ammonia-water solution) through unsaturated beds.

1. Introduction

Hydrodynamic dispersion plays an important role in an aquifer, such as in tracer responses, the migration of contamination, or the mixing of freshwater with salt water in a coastal aquifer. *Levenspiel* [1972] introduced an intensity of dispersion in saturated packed beds based on various experiments and concluded that the dispersion intensity was almost proportional to the mean axial velocity and the particle size. *Bear* [1972] also discussed a relationship between molecular diffusion and convective dispersion, using various experimental data on dispersion coefficients. Recently, *Gelhar et al.* [1992] reviewed field-scale dispersion coefficients in aquifers by summarizing the data obtained from 59 different field sites. These data were classified into three reliability classes by using the information regarding the experimental conditions on aquifer types, hydraulic properties, tracers, type of monitoring network, flow configuration, etc. The results demonstrated that longitudinal and transverse dispersivity tended to increase with the observation scale, and vertical transverse dispersivities were 1 order of magnitude smaller than horizontal transverse dispersivities.

Hydrodynamic dispersion coefficients for the unsaturated zone have not been sufficiently investigated, although practical values are needed for exploring NAPL (non–aqueous phase liquid) transport in an aquifer [*Crittenden et al.*, 1986; *Kueper and Frind*, 1991a, b; *Powers et al.*, 1991, 1992] and for designing remediation processes such as air sparging [*Unger et al.*, 1995; *Chen et al.*, 1996], bioventing [*Wilson*, 1995; *Anderson*, 1994, 1995] and soil vapor extraction [*Gierke et al.*, 1990, 1992; *Armstrong et al.*, 1994; *Conant et al.*, 1996; *Fischer et al.*, 1996]. In particular, there is little information available for cases in the range of high water saturation. In the range of relatively low water saturation, some studies of hydrodynamic dispersion have been reported. In unsteady unsaturated flow, transport of water and solutes during infiltration were investigated by *Kirda et al.* [1973, 1974], *de Smedt and Wierenga* [1978], *Smiles et al.* [1981], *Smiles and Gardiner* [1982], *Bond and Phillips* [1990], and others. Of them, *Smiles et al.* [1978], *White et al.* [1979], and *Laryea et al.* [1982] estimated solute dispersion coefficients as a function of the volumetric water content. For steady unsaturated flow *de Smedt and Wierenga* [1979a, b, 1984] and *Bond and Wierenga* [1990] reported the effects of mobile and immobile water fractions on solute transport, and *Mansell et al.* [1985, 1992] proposed mathematical models for predicting reactions and transport of phosphorus. *Wilson and Gelhar* [1981] developed an analytical technique for evaluating solute displacement in unsaturated soils. *Butters et al.* [1989] and *Butters and Jury* [1989] reported field-scale transport of bromide in an unsaturated zone and used the results to calibrate and to test various models of area-averaged solute transport. Recently, *Conca and Wright* [1990, 1991] obtained diffusion coefficients in gravel under unsaturated conditions. *Smiles et al.* [1995] investigated diffusion coefficients of tritium in arid disposal sites.

The purpose of this study was to investigate dispersion co-

Paper number 1998WR900111.
0043-1397/99/1998WR900111$09.00

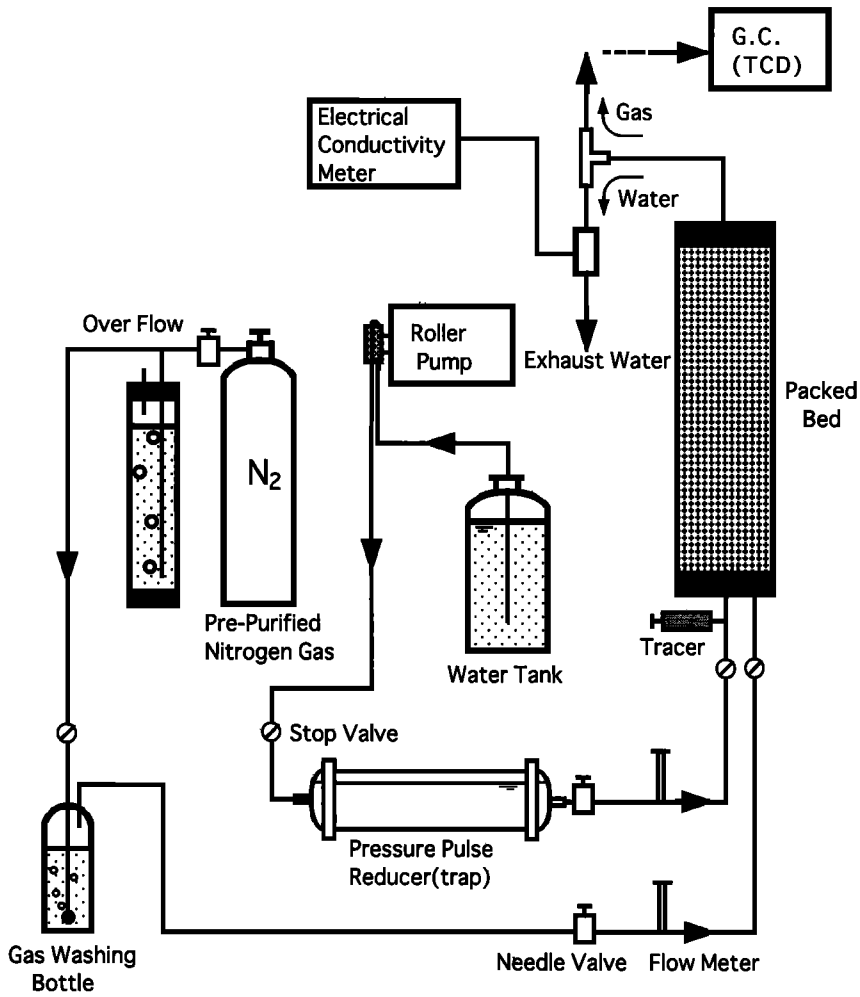

Figure 1. Schematic diagram of experimental apparatus.

efficients at relatively high values of water saturation, S_w, and to examine the relationship between the Peclet number, Pe, and water saturation by applying a one-dimensional advection-dispersion model to the experimental results through some packed beds. Furthermore, the relationship for two-phase flow was used to analyze the mass transport of the two-phase tracer (ammonia-water solution) through unsaturated beds using gas chromatography, which detected NH_3 gas content in gas phase at the outlet of the packed bed.

2. Experiments

Figure 1 shows a schematic diagram of the experimental apparatus. The packed bed was made from an acrylic cylinder 52.0 cm long and with an inside diameter of 4.1 cm, which was filled with glass beads with an average diameter of 0.1 cm. The column length (i.e., the length of the packed bed) was 50.0 cm. The permeability and porosity of the packed bed were 6.5×10^{-10} m^2 and 0.373, respectively. Deionized water was injected continuously into the bed from the bottom at a constant flow rate using a roller pump. To prevent a regular pulse caused by the pump, a trap containing water and air was placed between the pump and the bed. Nitrogen gas saturated with water vapor was continuously injected from the bottom, and the hydraulic head at the inlet of the bed was fixed by the overflow.

Tracer experiments were carried out under following three flow conditions: saturated water flow condition A, and the unsaturated flow conditions B and C. Figure 2a shows a conceptual illustration of condition A. The packed bed is saturated with water. Figure 2b shows condition B with entrapped gases. In condition B, only water flows continuously through the bed. Figure 2c shows a two-phase flow condition C, where almost all gases exist as mobile gases. Hereafter, conditions B and C are referred to as "unsaturated one-phase flow" and "unsaturated two-phase flow," respectively.

The water saturation in the bed was held within the range of 0.41–0.85 by controlling the flow rate of the gas phase. *Chen et al.* [1996] showed through their experiments and numerical simulation that water saturation became approximately uniform in the homogeneous bed as the continuous flow of water and gas became steady. The time required to obtain the steady state mainly depended on permeability of the column. The times were 1 min and 80 min for a packed beds of 1.1×10^{-10} m^2 (106 darcies) and 3.0×10^{-12} m^2 (3 darcies), respectively. On the basis of the results of *Chen et al.* [1996], the water injection and gas injection was continued for 1 hour in this study.

The packed bed was disconnected once in order to determine the water saturation by weighing the column after 1 hour. Figure 3 shows the gas flow velocity and water saturation at steady state. The average water saturation decreases as the gas

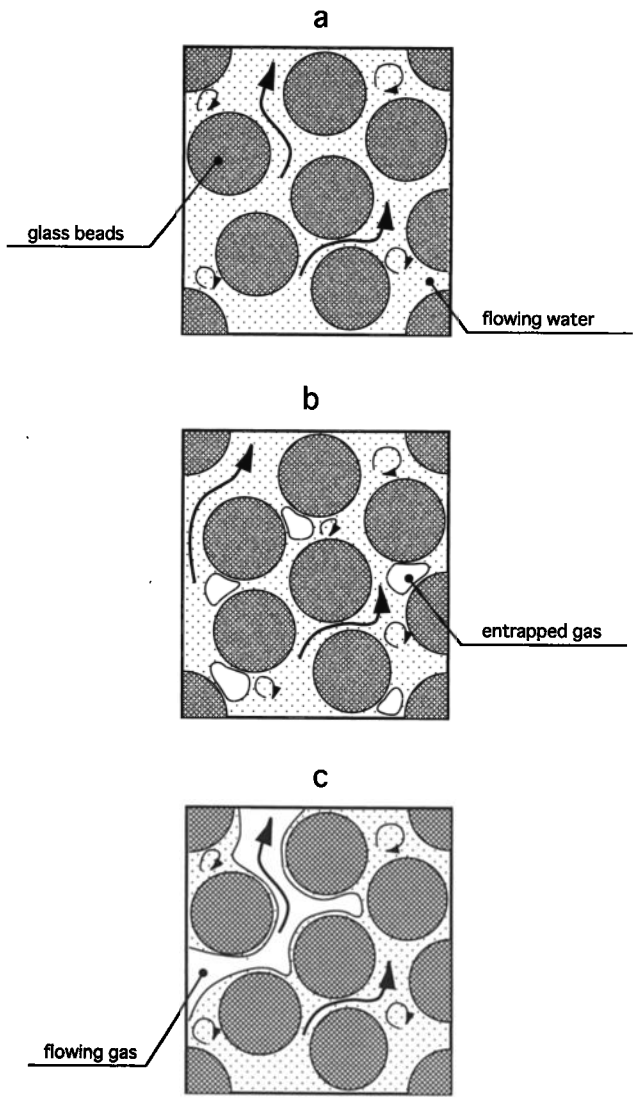

Figure 2. Schematic representations of the three different flow conditions through the bed: (a) saturated flow, (b) unsaturated one-phase flow with entrapped gases, and (c) unsaturated two-phase flow.

flow rate increases for any water flow rate. After measuring water saturation and continuing the injection of the water and gas for 1 hour, either 5.0 mL of KCl solution (0.1 mol/L) or 8.0 mL of an ammonia-water solution (about 28.0 wt% NH_4OH) was injected as a tracer with a syringe within a few seconds. The injection point was at the silicon tube, which was connected to the bed at the inlet. The actual concentration of the tracer at the inlet was calculated on the basis of the water flow rate, the concentration of the tracer in the syringe, and the injection time (5% and 10% of the space time for KCl and NH_4OH solutions, respectively). At the outlet an electrical conductivity meter (TOA Electronics; CM40V) measured the concentration of the KCl solution. When the ammonia-water solution was injected, the concentration in the water phase was measured the same as with the KCl solution. The NH_3 content in the exit gas was measured by gas chromatography (Yanako; G-3800) every 30 s. After obtaining the tracer responses, water saturation was measured again by weighing the column. If the two values for water saturation disagreed, the tracer test was treated as a failed run.

Figure 4a shows the relationship between the concentration of KCl solution and electrical conductivity, which increases linearly as the concentration of KCl solution increases. The electrical conductivity of the ammonia-water solution (Figure 4b) decreases as the concentration of the solution increases in the high range. Thus the tracer tests using NH_4OH were conducted with an effluent NH_4OH concentration of less than 2.0 mol/L.

3. Mathematical Model

3.1. Governing Equations

Mass transport of a nonreactive solute through unsaturated porous media in a one-dimensional system is usually analyzed with the following equation:

$$\frac{\partial(\varepsilon S_w c_w)}{\partial t} = \frac{\partial}{\partial z}\left(D_{hw}\frac{\partial c_w}{\partial z}\right) - \frac{\partial(u_w c_w)}{\partial z} \tag{1}$$

where c_w is the solute concentration in the water (mol/m^3), S_w is the water saturation (m^3/m^3), ε is the porosity of the porous medium, u_w is the Darcy flux (m/s) of the water, D_{hw} is the hydrodynamic dispersion coefficient (m^2/s) of the solute in the water phase, t is time (s), and z is the space coordinate (m). Using (1), *Kirda et al.* [1973], *Bresler* [1973], *Bresler and Laufer* [1974], and *Yule and Gardner* [1978] have shown that D_{hw} in unsaturated beds was larger than that in saturated beds. Equation (1) can be written as

$$\varepsilon S_w \frac{\partial c_w}{\partial t} = D_{hw}\frac{\partial^2 c_w}{\partial z^2} - u_w\frac{\partial c_w}{\partial z} \tag{2}$$

for steady state flow through a uniform porous medium with a uniform water content distribution. The dimensionless form of (2) is

$$\frac{\partial C_w}{\partial T} = \frac{\zeta}{Pe}\frac{\partial^2 C_w}{\partial Z^2} - \frac{\partial C_w}{\partial Z} \tag{3}$$

where $Z = z/L$, $C_w = (c_w - c_b)/(c_{w0} - c_b)$, $T = t/t^*$, and $\zeta = d_p/L$; c_b is the background concentration, t^* is the space time ($= L\varepsilon S_w/u_w$), ζ is the ratio of d_p to L ($\zeta = 0.002$ in this study), d_p is the particle diameter (m), and L is the length of the column (m). Pe is the Peclet number defined by

$$Pe = \frac{d_p(u_w/\theta_w)}{(D_{hw}/\theta_w)} = \frac{d_p u_w}{D_{hw}} \qquad \theta_w = \varepsilon S_w \tag{4}$$

where θ_w is the volumetric fraction of the water phase. In this study (3) is used to describe the advection and dispersion of KCl solution through an unsaturated porous medium.

When the ammonia-water solution is injected from the bottom, molecular ammonia (NH_3) and ammonium ion (NH_4^+) coexist in the water phase. The NH_3 is transferred from the water phase to the gas phase and vice versa. Gas-phase concentration of NH_3 exists in equilibrium with water-phase concentration of NH_3 at the interface between the water and the gas. When we consider mass transfer for a three-phase system in which the volume fraction of solid, liquid, and gas are constant, the flow equations are expressed as

$$\varepsilon S_w \frac{\partial c_w}{\partial t} = D_{hw}\frac{\partial^2 c_w}{\partial z^2} - u_w\frac{\partial c_w}{\partial z} + k_0(c_g - Hc_w) \tag{5}$$

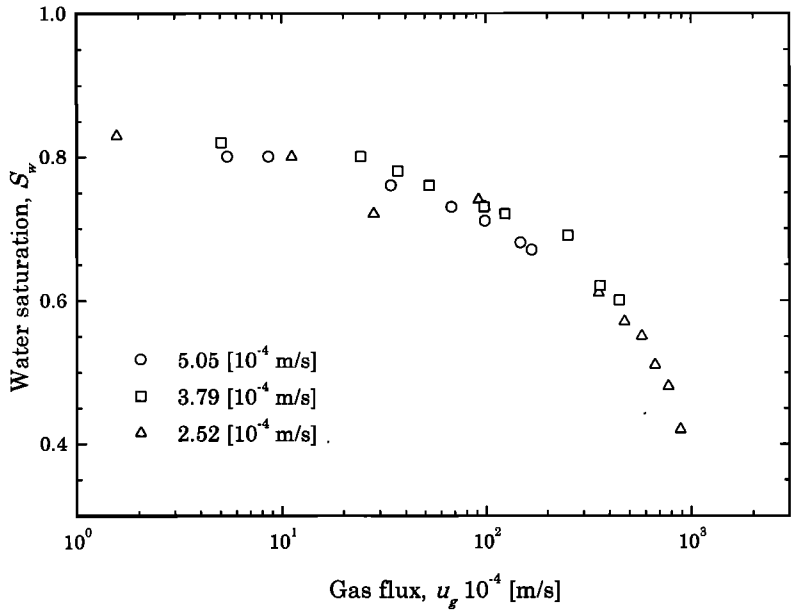

Figure 3. Relationship between the gas flow rate and water saturation in a steady state.

$$\varepsilon S_g \frac{\partial c_g}{\partial t} = D_{hg} \frac{\partial^2 c_g}{\partial z^2} - u_g \frac{\partial c_g}{\partial z} - k_0(c_g - Hc_w) \qquad (6)$$

where S_w and S_g are water and gas saturation, respectively ($S_w + S_g = 1$), k_0 is the mass transfer coefficient across the air-water interface, and H is the dimensionless Henry's constant. The subscripts w and g indicate the water phase and gas phase, respectively. H is modified in relation to the pressure gradient. The ammonia-water solution does not conform to Henry's law for a change in water density owing to its strong solubility. Therefore H in (5) and (6) is determined along with its modification for the water density. An effect of gas-pressure gradient on Henry's constant is neglected because the gas-pressure gradient was small, around 0.2 atm, in the tracer tests with ammonia-water solution. Under the pressure gradient the modification for the pressure gradient is small. The flux of the dispersion in the gas phase, that is, $-D_{hg}[(\partial c_g)/(\partial z)]$, is much smaller than the gas flux, that is, u_g in (6). Therefore the dispersion term in (6) is negligible [*Niibori et al.*, 1992; *Niibori and Chida*, 1994]. The dimensionless forms of (5) and (6) are

$$\frac{\partial C_w}{\partial T} = \frac{\zeta}{Pe} \frac{\partial^2 C_w}{\partial Z^2} - \frac{\partial C_w}{\partial Z} + \frac{S_t}{\zeta}(C_g - HC_w) \qquad (7)$$

$$\Gamma \frac{\partial C_g}{\partial T} = -U_g \frac{\partial C_g}{\partial Z} - \frac{S_t}{\zeta}(C_g - HC_w) \qquad (8)$$

where $C_g = c_g/c_{w0}$, $\Gamma = S_g/S_w$, and $U_g = u_g/u_w$. S_t is the Stanton number ($S_t = k_0 d_p/u_w$), which is the ratio of the mass transfer rate to the advection rate.

The boundary conditions are

$$C_{w-} = C_{w+} - \frac{\zeta}{Pe} \frac{\partial C_w}{\partial Z}\bigg|_{Z=0+} \qquad Z = 0 \qquad (9)$$

$$\frac{\partial C_w}{\partial Z} = 0 \qquad Z = 1 \qquad (10)$$

where C_{w^-} and C_{w^+} are the tracer concentrations at $Z = 0^-$ and $Z = 0^+$, respectively. Equation (9) is the so-called closed-

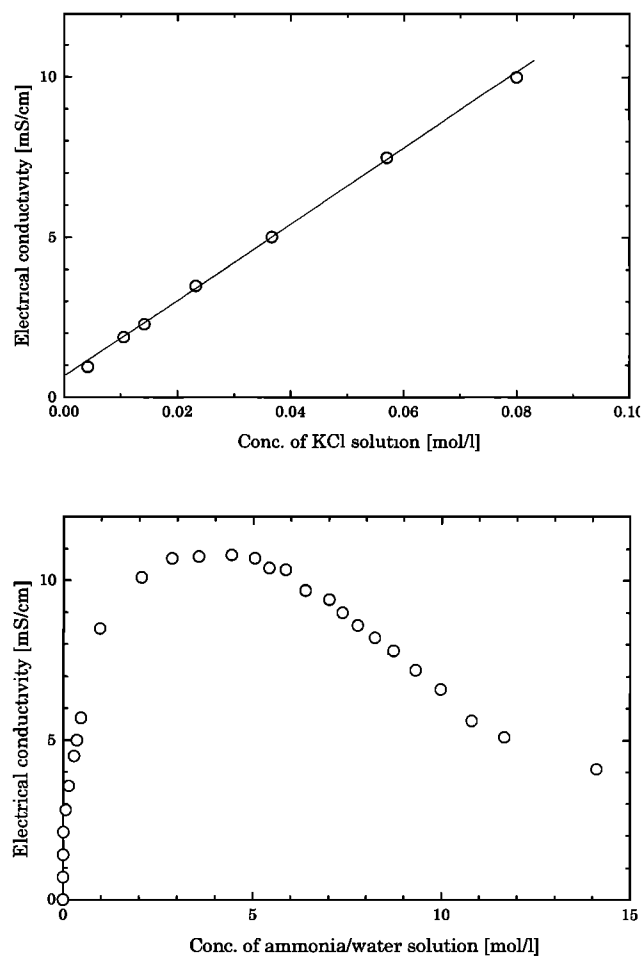

Figure 4. Relationship between concentration of tracers and electrical conductivity. (a) KCl solution. The fitted equation is $y = 118.89 \times -0.61$, where y and x are the electrical conductivity (mS/cm) and concentration of the KCl solution (mol/l), respectively. (b) Ammonia-water solution.

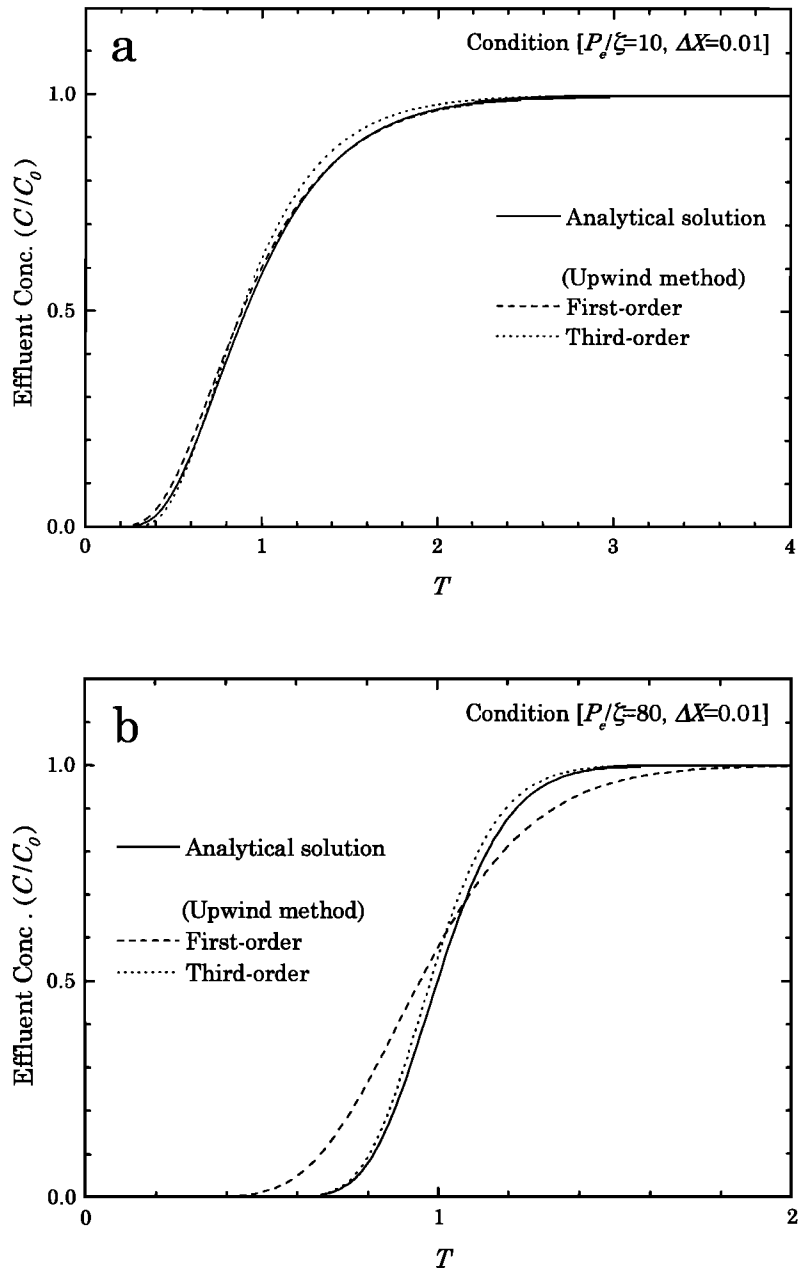

Figure 5. Comparison of the analytical solution and numerical results: (a) $Pe/\zeta = 10$ and (b) $Pe/\zeta = 80$. The analytical solutions were obtained by equation (23). The numerical results were calculated using the upwind methods.

vessel boundary condition, which is applicable to a system which has a larger backmixing magnitude than the surroundings, for example, at the inlet of the column [*Wehner and Wilhelm*, 1956; *Levenspiel*, 1972].

The initial conditions and tracer injection are described by

At $0 < Z < 1$

$$T = 0 \qquad C_w = 0 \qquad C_g = 0 \tag{11}$$

$Z = 0$

$$0 < T < T_{in} \qquad C_{w^-} = 1 \tag{12}$$

$Z = 0$

$$T < 0 \qquad T_{in} < T \qquad C_{w^-} = 0 \tag{13}$$

where T_{in} is the injection time of the tracer.

3.2. Numerical Solution of Governing Equations

Equations (3), (7), (8), and (9)–(13) were solved using a FTCS (forward time central space) finite difference method. In discretizing the advection terms in (3), (7), and (8), the third-order upwind difference method was applied (see appendix). Figure 5 shows the numerical and analytical solutions of (3) under the following initial condition:

$$C_{w|Z=0} = \begin{cases} 0 & -\infty < T < 0 \\ C_0 & 0 < T < \infty \end{cases} \tag{14}$$

The numerical calculations are based on the first- and third-order upwind methods. When $Pe/\zeta = 10$ (Figure 5a), the two

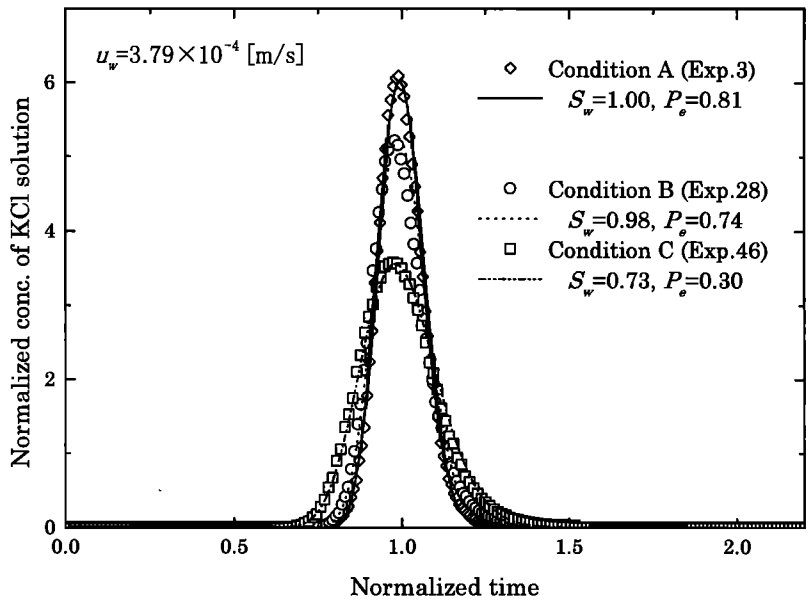

Figure 6. Observed and calculated breakthrough curves for the three different flow conditions. The numerical curves were calculated using equation (3), and the value of Pe under each condition was obtained.

Table 1. Experimental Conditions and Results of the Breakthrough Curve Fitting for the Tracer Tests, Conditions A and B

Experiment	Water Saturation, S_w	Water Content, θ_w	Water Flux, u_w, 10^{-4} [m/s]	Pore Water Velocity, u_w/θ_w, 10^{-4} [m/s]	Peclet Number, Pe	Dispersion Coefficient, D_{hw}, 10^{-6} [m^2/s]
			Saturated Water Flow, Condition A			
1	1.00	0.37	2.17	5.95	0.78	0.46
2	1.00	0.37	3.26	8.92	0.74	0.73
3	1.00	0.37	3.79	11.48	0.81	0.92
4	1.00	0.37	4.77	13.07	0.76	1.05
5	1.00	0.37	5.45	14.94	0.76	1.20
6	1.00	0.37	5.76	15.77	0.77	1.25
7	1.00	0.37	6.51	17.85	0.73	1.49
8	1.00	0.37	8.88	24.34	0.72	2.06
9	1.00	0.37	10.45	28.64	0.73	2.39
10	1.00	0.37	2.42	6.64	0.75	0.54
11	1.00	0.37	2.58	7.06	0.81	0.53
12	1.00	0.37	2.73	7.47	0.87	0.52
13	1.00	0.37	5.15	14.11	0.86	1.00
14	1.00	0.37	5.23	14.32	0.85	1.02
15	1.00	0.37	4.32	11.83	0.80	0.90
16	1.00	0.37	3.33	9.13	0.80	0.69
17	1.00	0.37	2.05	5.60	0.74	0.46
18	1.00	0.37	2.58	7.06	0.79	0.54
19	1.00	0.37	6.06	16.60	0.80	1.26
20	1.00	0.37	6.89	18.88	0.80	1.44
21	1.00	0.37	7.73	21.17	0.82	1.57
22	1.00	0.37	1.36	3.74	0.85	0.27
			Unsaturated Single-Phase Flow With Entrapped Gases, Condition B			
23	0.76	0.28	2.52	8.86	0.56	0.45
24	0.81	0.30	2.52	8.34	0.56	0.45
25	0.82	0.30	2.52	8.30	0.56	0.45
26	0.86	0.32	2.52	7.86	0.57	0.44
27	0.98	0.37	2.52	6.91	0.72	0.35
28	0.98	0.37	3.79	10.36	0.74	0.49
29	0.84	0.31	3.79	12.03	0.66	0.57
30	0.80	0.30	3.79	12.77	0.64	0.59
31	0.77	0.29	3.79	13.22	0.59	0.64
32	0.98	0.37	5.05	13.81	0.84	0.60
33	0.89	0.33	5.05	15.28	0.75	0.68
34	0.87	0.32	5.05	15.60	0.73	0.69
35	0.84	0.31	5.05	16.14	0.70	0.72
36	0.78	0.29	5.05	17.38	0.65	0.78

Table 2. Experimental Conditions and Results of the Breakthrough Curve Fitting for the Tracer Tests, Condition C

Experiment	Water Saturation, S_w	Water Content, θ_w	Water Flux, u_w, 10^{-4} [m/s]	Pore Water Velocity, u_w/θ_w, 10^{-4} [m/s]	Gas Flux, u_w, 10^{-4} [m/s]	Pore Gas Velocity, u_w/θ_g, 10^{-4} [m/s]	Peclet Number, Pe	Dispersion Coefficient, D_{hw}, 10^{-6} [m^2/s]
37	0.73	0.27	2.52	9.33	98.55	962.90	0.27	0.94
38	0.74	0.28	2.52	9.15	91.81	945.27	0.27	0.94
39	0.72	0.27	2.52	9.45	28.11	265.86	0.32	0.80
40	0.80	0.30	2.52	8.43	11.15	151.39	0.41	0.62
41	0.83	0.31	2.52	8.20	1.57	24.06	0.48	0.53
42	0.82	0.30	3.79	12.46	5.06	73.36	0.54	0.70
43	0.80	0.30	3.79	12.68	24.31	327.56	0.40	0.95
44	0.78	0.29	3.79	13.08	36.57	437.71	0.36	1.05
45	0.76	0.28	3.79	13.32	52.58	593.52	0.34	1.11
46	0.73	0.27	3.79	13.83	97.65	984.15	0.30	1.26
47	0.72	0.27	3.79	14.18	123.97	1170.24	0.30	1.26
48	0.67	0.25	5.05	20.18	168.31	1371.56	0.28	1.83
49	0.68	0.25	5.05	19.97	148.13	1233.31	0.27	1.90
50	0.71	0.26	5.05	19.11	98.76	907.65	0.28	1.80
51	0.73	0.27	5.05	18.46	67.69	680.18	0.33	1.52
52	0.76	0.28	5.05	17.78	33.93	381.60	0.37	1.37
53	0.80	0.30	5.05	17.00	8.61	113.31	0.55	0.92
54	0.80	0.30	5.05	16.97	5.42	71.75	0.56	0.91
55	0.55	0.21	2.57	12.46	575.02	3441.06	0.14	1.83
56	0.51	0.19	2.52	13.19	666.03	3666.56	0.14	1.80
57	0.57	0.21	2.52	11.94	473.65	2932.63	0.15	1.68
58	0.61	0.23	2.55	11.17	354.98	2452.82	0.16	1.59
59	0.69	0.26	3.79	14.78	252.48	2162.56	0.29	1.31
60	0.62	0.23	3.79	16.27	361.17	2575.21	0.24	1.58
61	0.60	0.22	3.79	17.06	446.38	2954.88	0.21	1.80
62	0.48	0.18	2.40	13.51	772.83	3954.07	0.13	1.85
63	0.41	0.15	2.40	15.68	883.67	4015.40	0.10	2.40

numerical calculations and the analytical solution show good agreement. For $Pe/\zeta = 80$ (Figure 5b) the response using the first-order upwind method is clearly different from the analytical solution, while the result using the third-order upwind method agrees with the analytical solution. This is due to numerical dispersion resulting from applying the upwind method to the advective term. In this study the values of Pe/ζ are larger than 80. Thus the third-order upwind method was used for the numerical calculation of the governing equations.

4. Results and Discussion

4.1. Hydrodynamic Dispersion in Porous Media

Figure 6 compares the experimental and numerical results, where the longitudinal axis and the horizontal axis show the normalized concentration of the KCl solution and normalized time, respectively. In this figure the values of S_w are 1.0, 0.94, and 0.73 for conditions A, B, and C (see Figure 2), respectively. The value of u_w is 3.79×10^{-4} m/s. The parameters in the

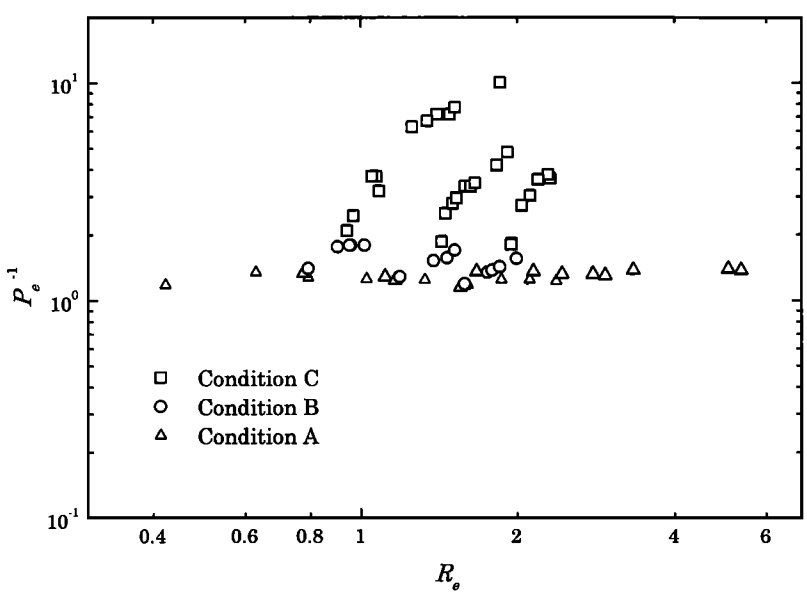

Figure 7. Relationship between the Peclet number and the Reynolds number. Triangles represent results under saturated condition in the column. Circles and squares are the results under unsaturated single- and two-phase condition, respectively.

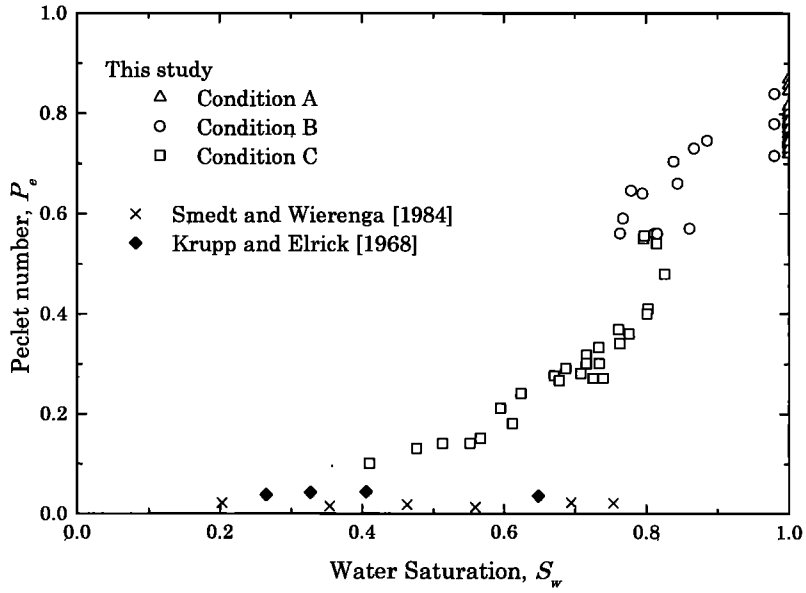

Figure 8. Relationship between the Peclet number and the water saturation. Open symbols are the results of this study. Solid diamonds and crosses are the results of *Krupp and Elrick* [1968] and *Smedt and Wierenga* [1984], respectively. The values of the Peclet numbers were calculated on the basis of the theory of *Smedt and Wierenga* [1984].

equations are Pe, ζ, and T_{in}. On the basis of the experimental conditions, the value of ζ and T_{in} are 0.02 and 0.05, respectively. The only unknown parameter in the mathematical model is Pe. These values were determined on the basis of several trials to fit the data. Figure 6 shows good agreement when the Pe is 0.81, 0.74, and 0.30 for flow conditions A, B, and C, respectively. These results show that Pe decreases as S_w decreases. To determine the effect of S_w on Pe, additional tracer experiments were conducted for different values of S_w. The experimental conditions are shown in Tables 1 and 2.

Figure 7 shows the relationship between $1/Pe$ and Re for the three flow conditions as shown by *Levenspiel* [1972] in saturated flow conditions, where Re is the Reynolds number defined as $Re = u_w\rho_w d_p/(\mu_w\theta_w)$. In the tracer experiments for conditions B and C, u_w was set at between 1.36×10^{-4} m/s and 10.45×10^{-4} m/s. Many investigations have already shown that under saturated flow conditions, $1/Pe$ is almost constant, with a value ranging from 1.0 to 2.0 for any value of Re in a laminar flow. For condition A the values of $1/Pe$ range from 1.15 to 1.39. The values of $1/Pe$ for condition B are larger than those for condition A, while condition C shows the largest $1/Pe$ values.

Figure 8 shows the Peclet number as a function of water saturation for the conditions A, B, and C. Condition A is the saturated flow condition. Conditions B and C are the single-phase flow with entrapped gases and two-phase flow, respectively. For condition A the values of Pe are in the range of 0.75 to 0.87. For condition B Pe decreases linearly as S_w decreases. For condition C the rate of the decrease in Pe is different from that in B. Pe declines sharply at S_w values of 0.83–0.75 but declines gradually as S_w decreases at S_w values of 0.75–0.41. Figure 8 also shows the experimental results of *Krupp and Elrick* [1968] and *de Smedt and Wierenga* [1984]. Although their experimental conditions were not similar to those in this study (with regard to tracers, particle diameter, column length, and water flow velocity, as shown in Table 3), the Pe in this study seems to approach their data as S_w decreases.

Levenspiel [1972] showed that the Pe defined as (4) took a constant value for any value of u_w and d_p because D_h was almost proportional to u_w and d_p. By using Pe defined in this way, effects of variation of u_w and d_p on Pe can be negligible. However, it has not been clarified yet whether the trend under the unsaturated condition holds or not. The relationship among Pe, S_w, and Re was examined by using the equation $Pe = a(S_w)^n(Re)^m$, where a, n, and m were constant. The results were that the value of m was below 0.2; therefore Re was neglected. The following two mathematical relationships were obtained from the data using the least squares method:

For single-phase flow

$$Pe = 0.8S_w^{1.2} \tag{15}$$

For two-phase flow

$$Pe = 0.9S_w^{3.1} \tag{16}$$

Figure 9 shows the experimental values and the mathematical relationships between Pe and S_w.

Table 3. Experimental Conditions in This Study and in Those of *Krupp and Elrick* [1968] and *Smedt and Wierenga* [1984]

	Tracer	Particle Diameter, d_p, mm	Column Length, L, m	Darcy Flow Velocity, u_w, m/s
This study	KCl	1.0	0.5	1.36×10^{-4} to 10.45×10^{-4}
Krupp and Elrick	$CaCl_2$	0.1	0.3	5.67×10^{-7} to 7.74×10^{-6}
Smedt and Wierenga	$CaCl_2$	0.1	0.1	1.62×10^{-7} to 2.67×10^{-5}

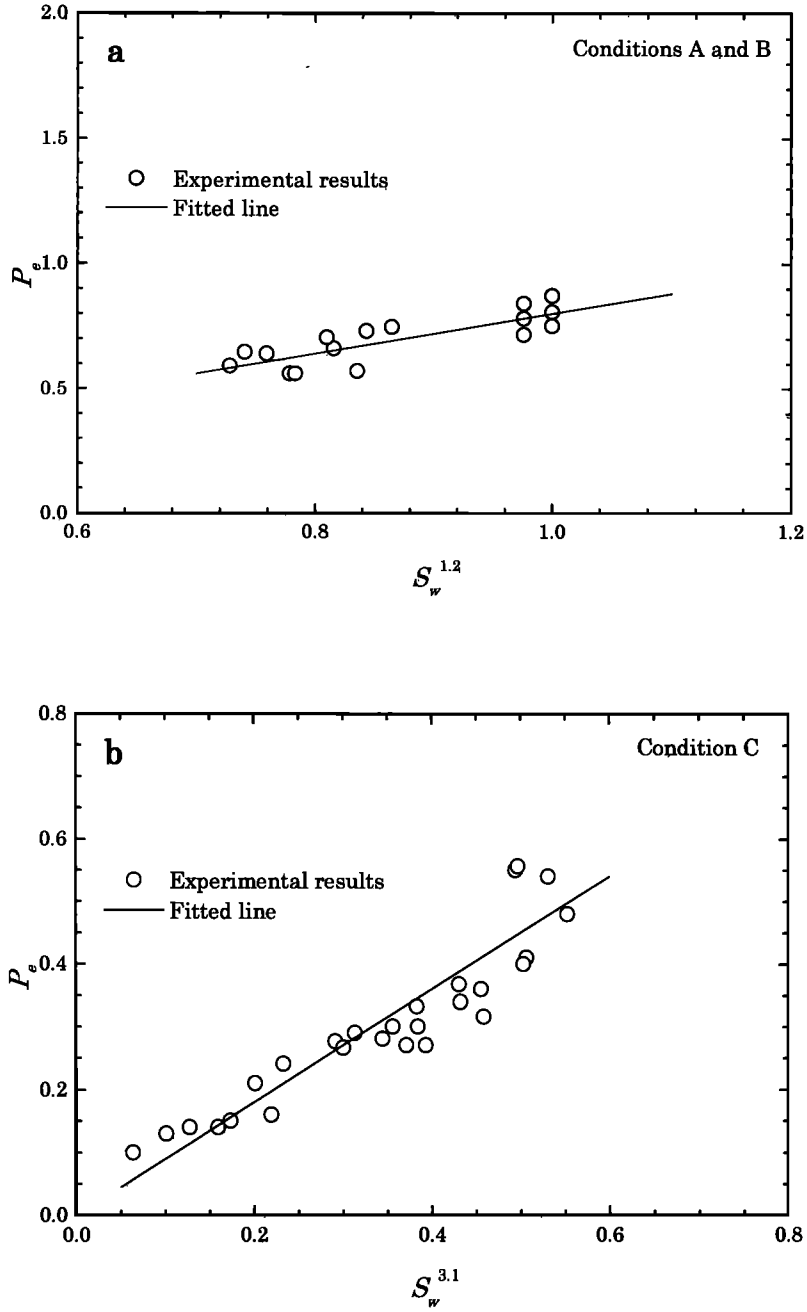

Figure 9. Experimental results and fitted lines by the least squares method: (a) One-phase flow experiments (conditions A and B) and (b) Two-phase flow experiments (condition C). The fitted equations for Figures 9a and 9b are shown in equations (14) and (15), respectively.

4.2. Application to Mass Transport of the Two-Phase Tracer

The results of the tracer experiments using the KCl solution provided the relationship between the Peclet number and water saturation, which was used to analyze the mass transport of the two-phase tracer through unsaturated beds. The breakthrough curves of the water phase and the gas phase were compared with the calculated results using the numerical model, in which the only unknown parameter was S_t, because (15) gave a value of Pe for each S_w.

Figure 10 shows the sensitivity of S_t to the variation in the dimensionless concentration at the outlet and the experimental response at $S_w = 0.74$. When S_t is greater than 5, the response does not depend upon S_t, while the sensitivity decreases as the value of S_t increases. There is good agreement between the experimental and numerical results for $S_t > 5$. This result shows that the rate of mass transfer of NH_3 through the films was large compared with the fluxes associated with the water- and gas-phase flow. On the basis of these calculations and the experimental response, S_t is assumed to be 10 in the numerical analysis.

As mentioned above, two values of the parameters were evaluated in advance. The value of the Peclet number was determined by (16), and the value of the Stanton number was estimated as 10. Figure 11 shows the calculated breakthrough curves and experimental data of a tracer for $S_w = 0.80$ and 0.82. (Figure 11a shows responses for the gas phase, and Figure

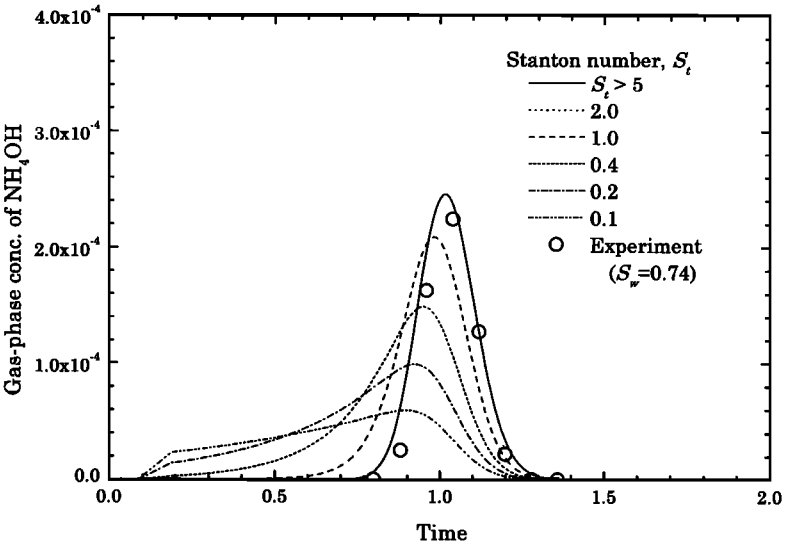

Figure 10. Sensitivity of S_t, and an experimental response ($S_w = 0.74$, $Pe = 0.35$).

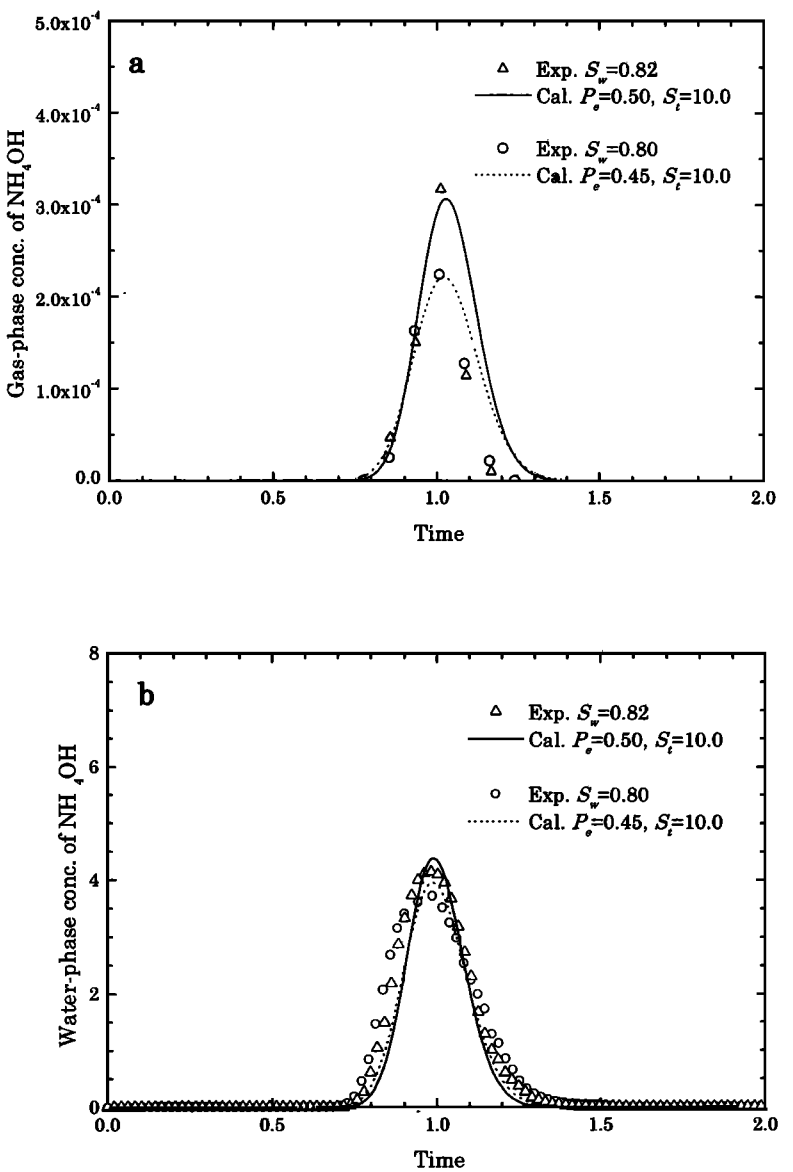

Figure 11. Comparisons of the numerical and experimental results: (a) responses for the gas phase and (b) responses for the water phase.

11b shows responses for the water phase). The numerical results agree well with the experimental results without any fitting parameter and therefore support the validity of the relationship between Pe and S_w.

5. Conclusion

Hydrodynamic dispersion coefficients were experimentally determined at relatively high values of water saturation. The results gave a relationship between the Peclet number and water saturation. A critical water saturation was observed, which depended on whether or not the gas phase in the bed was mobile. Above the critical saturation, there was unsaturated one-phase flow, and Pe linearly decreased as S_w decreased. Below the critical saturation, water- and gas-phase flow appeared. The relationship was characterized by a steep decrease in Pe as S_w decreased within the range of 0.83–0.75, followed by a gradual decline within the range of 0.75–0.41.

The Pe obtained in this study for saturated flow was in the range of 0.75–0.87, which agrees with the value reported by many investigations. For unsaturated one-phase flow the value of Pe ranged from 0.56, at a water saturation of 0.76, to 0.84, at a water saturation of 0.98. Unsaturated two-phase flow showed Pe values ranging from 0.10 at $S_w = 0.41$ to 0.56 at $S_w = 0.83$. In the range of u_w used in this study the dependence of Re on Pe was slight. Thus two mathematical relationships between Pe and S_w for both unsaturated flow conditions were determined from the experimental data. The equations revealed that Pe for unsaturated single-phase flow was proportional to S_w to the 1.2th power, while Pe for unsaturated two-phase flow was proportional to S_w to the 3.1th power. Furthermore, the relationship for two-phase flow was applied to the two-phase tracer (ammonia-water solution) experiments. Using the above relationship, the numerical model well expresses the experimental responses for both the water phase and the gas phase with no fitting parameter.

Appendix

To explain the third-order upwind method, we rewrite (3) using

$$\frac{\partial C}{\partial T} = \frac{1}{Pe'}\frac{\partial^2 C}{\partial Z^2} - U\frac{\partial C}{\partial Z} \tag{17}$$

where Pe/ζ in (3) is replaced by Pe', C is the concentration, Z is the space coordinate, U is the velocity, and T is time. In discretizing the equation we use the so-called upwind method for the advection term. The finite difference equation for the advective term by the first-order upwind method is expressed as

$$U\frac{\partial C}{\partial Z}\bigg|_{Z=Z_i} = \begin{cases} \dfrac{U_i(C_i - C_{i-1})}{\Delta Z} & U_i > 0 \\ \dfrac{U_i(C_{i+1} - C_i)}{\Delta Z} & U_i < 0 \end{cases} \tag{18}$$

where i is the finite difference counter in Z. Equation (18) can be rewritten as

$$U\frac{\partial C}{\partial Z}\bigg|_{Z=Z_i} = U_i\frac{C_{i+1} - C_{i-1}}{2\Delta Z} - \frac{|U_i|\Delta Z}{2}\frac{C_{i+1} - 2C_i + C_{i-1}}{(\Delta Z)^2} \tag{19}$$

In this equation the first term on the right side is the central space difference term of the advection term. The second term on the right side is not a truncation error from a Taylor expansion but rather a discretization error, which is called the "numerical dispersion term." This term is proportional to the finite difference equation of a second differential term by ΔZ and the absolute value of U_i. Here (17) has a second differential term, and the finite difference equation of the right side of (17) is given as

$$\left(\frac{1}{Pe}\frac{\partial^2 C}{\partial Z^2} - U\frac{\partial C}{\partial Z}\right)\bigg|_{Z=Z_i} = \left(\frac{1}{Pe} + \frac{|U_i|\Delta Z}{2}\right) \cdot \frac{C_{i+1} - 2C_i + C_{i-1}}{(\Delta Z)^2} - U_i\frac{C_{i+1} - C_{i-1}}{2\Delta Z} \tag{20}$$

This indicates that for a large value of ΔZ or for a large value of Pe', we cannot neglect the numerical dispersion term. The third-order upwind method is advantageous for reducing the numerical error at a large value of Pe' [*Kobayashi*, 1995]. The difference equation of the advection term is given as

$$U\frac{\partial C}{\partial T}\bigg|_{Z=Z_i} = U_i\frac{-C_{i+2} + 8(C_{i+1} - C_{i-1}) + C_{i-2}}{12\Delta Z} + \frac{|U_i|(\Delta Z)^3}{12}\frac{C_{i+2} - 4C_{i+1} + 6C_i - 4C_{i-1} + C_{i-2}}{(\Delta Z)^4} \tag{21}$$

In using the third-order method the advection term is discretized to the central space difference equation, which is fourth-order, and the error term. The second term on the right side, that is, the error term, is proportional to the finite difference equation of a fourth differential term by the absolute value of U_i and the third power of ΔZ. The numerical error is thus reduced to third order.

For example, let us consider (17) based on the upwind methods under the initial condition

$$C|_{Z=0} = \begin{cases} 0 & -\infty < T < 0 \\ C_0 & 0 < T < \infty \end{cases} \tag{22}$$

where the analytical solutions of (17) and (22) are [*Lapidus and Amundson*, 1952]

$$C_e(T) = \frac{C_0}{2}\left[\operatorname{erfc}\left\{(1 - T)\sqrt{\frac{Pe'}{4T}}\right\} + \exp(Pe')\operatorname{erfc}\left\{(1 + T)\sqrt{\frac{Pe'}{4T}}\right\}\right] \tag{23}$$

where C_e is the effluent solute concentration. The results are shown in Figure 4.

Notation

- c_b background water phase concentration, mol/m^3.
- c_e effluent concentration, mol/m^3.
- c_g gas-phase concentration, mol/m^3.
- c_w water-phase concentration, mol/m^3.
- c_{w0} initial concentration in the water phase at the inlet, mol/m^3.
- C_g dimensionless gas-phase concentration.
- C_w dimensionless water-phase concentration.

C_0 dimensionless concentration at the inlet.
d_p particle diameter, m.
D_{hg} gas-phase hydrodynamic dispersion coefficient, m^2/s.
D_{hw} water-phase hydrodynamic dispersion coefficient, m^2/s.
D_m molecular diffusivity, m^2/s.
H dimensionless Henry's constant.
k_0 mass transfer coefficient, s^{-1}.
L column length, m.
Pe Peclet number, equal to $u_w d_p/D_{hw}$.
Re Reynolds number, equal to $\rho_w u_w d_p/\mu_w \theta_w$.
S_g gas-phase saturation.
S_t Stanton number, equal to $k_0 d_p/u_w$.
S_w water-phase saturation.
t time, s.
t_1 average residence time, s.
t^* space time, s, equal to $\varepsilon S_w L/u_w$.
T dimensionless time.
T_{in} injection time, s.
u_g flow velocity of the gas phase, m/s.
u_w flow velocity of the water phase, m/s.
U_g dimensionless flow velocity of the gas phase, u_g/u_w.
z space coordinate, m.
Z dimensionless space coordinate.
ε porosity.
μ_w water-phase viscosity, g/m s.
θ_w volumetric fraction of the water phase.
Γ ratio of S_g to S_w.
ρ_w water-phase density, g/m^3.
ζ ratio of d_p to L.

References

Anderson, W. C. (Ed.), *Innovative Site Remediation Technology*, vol. 1, *Bioremediation*, Springer-Verlag, New York, 1994.

Anderson, W. C. (Ed.), *Innovative Site Remediation Technology*, vol. 8, *Vacuum Vapor Extraction*, Springer-Verlag, New York, 1995.

Armstrong, J. E., E. O. Frind, and R. D. McClellan, Nonequilibrium mass transfer between the vapor, aqueous, and solid phases in unsaturated soils during vapor extraction, *Water Resour. Res.*, *30*(2), 355–368, 1994.

Bear, J., *Dynamics of Fluids in Porous Media*, Elsevier, New York, 1972.

Bond, W. J., and I. R. Philips, Cation exchange isotherms obtained with batch and miscible displacement techniques, *Soil Sci. Soc. Am. J.*, *54*, 722–728, 1990.

Bond, W. J., and P. J. Wierenga, Immobile water during solute transport in unsaturated sand columns, *Water Resour. Res.*, *26*(10), 2475–2481, 1990.

Bresler, E., Anion exclusion and coupling effects in nonsteady transport through unsaturated soils, I, Theory, *Soil Sci. Soc. Am. Proc.*, *37*, 663–669, 1973.

Bresler, E., and A. Laufer, Anion exclusion and coupling effects in non-steady transport through unsaturated soils, II, Laboratory and numerical experiments, *Soil Sci. Soc. Am. Proc.*, *38*, 213–218, 1974.

Butters, G. L., and W. A. Jury, Field scale transport of bromide in an unsaturated soil, 2, Dispersion modeling, *Water Resour. Res.*, *25*(7), 1583–1589, 1989.

Butters, G. L., W. A. Jury, and F. F. Ernst, Field scale transport of bromide in an unsaturated soil, 1, Experimental metrology and results, *Water Resour. Res.*, *25*(7), 1575–1581, 1989.

Chen, M.-R., R. E. Hinkley, and J. E. Killough, Computed tomography imaging of air sparging in porous media, *Water Resour. Res.*, *32*(10), 3013–3024, 1996.

Conant, B. H., R. W. Gillham, and C. A. Mendoza, Vapor transport of trichloroethylene in the unsaturated zone: Field and numerical modeling investigations, *Water Resour. Res.*, *32*(1), 9–22, 1996.

Conca, J. L., and J. Wright, Diffusion coefficients in gravel under unsaturated conditions, *Water Resour. Res.*, *26*(5), 1055–1066, 1990.

Conca, J. L., and J. Wright, Aqueous diffusion coefficients in unsaturated materials, *Mater. Res. Soc. Symp. Proc.*, *212*, 879–884, 1991.

Crittenden, J. C., N. J. Hutzler, and D. G. Geyer, Transport of organic compounds with saturated groundwater flow: Model development and parameter sensitivity, *Water Resour. Res.*, *22*(3), 271–284, 1986.

de Smedt, F., and P. J. Wierenga, Approximate analytical solution for solute flow during infiltration and redistribution, *Soil Sci. Soc. Am. J.*, *42*, 407–412, 1978.

de Smedt, F., and P. J. Wierenga, Mass transfer in porous media with immobile water, *J. Hydrol.*, *41*, 59–67, 1979a.

de Smedt, F., and P. J. Wierenga, A generalized solution for solute flow on soils with mobile and immobile water, *Water Resour. Res.*, *15*(5), 1137–1141, 1979b.

de Smedt, F., and P. J. Wierenga, Solute transfer through columns of glass beads, *Water Resour. Res.*, *20*(2), 225–232, 1984.

Fischer, U., R. Schulin, M. Keller, and F. Stauffer, Experimental and numerical investigation of soil vapor extraction, *Water Resour. Res.*, *32*(12), 3413–3427, 1996.

Gelhar, L. W., C. Welty, and K. R. Rehfeldt, A critical review of data on field-scale dispersion in aquifers, *Water Resour. Res.*, *28*(7), 1955–1974, 1992.

Gierke, J. S., N. J. Hutzler, and J. C. Crittenden, Modeling the movement of volatile organic chemicals in columns of unsaturated soil, *Water Resour. Res.*, *26*(7), 1529–1547, 1990.

Gierke, J. S., N. J. Hutzler, and D. B. McKenzie, Vapor Transport in unsaturated soil columns: Implications for vapor extraction, *Water Resour. Res.*, *28*(2), 323–335, 1992.

Kirda, C., D. R. Nielsen, and J. W. Biggar, Simultaneous transport of chloride and water during infiltration, *Soil Sci. Soc. Am. Proc.*, *37*, 339–345, 1973.

Kirda, C., D. R. Nielsen, and J. W. Biggar, The combined effects of infiltration and redistribution on leaching, *Soil Sci.*, *117*(6), 323–330, 1974.

Kobayashi, T., *Analysis of Incompressible Flows, Comput. Fluid Dyn. Ser.*, vol. 1, edited by T. Kobayashi, Univ. of Tokyo Press, Tokyo, 1995.

Krupp, H. K., and D. E. Elrick, Miscible displacement in an unsaturated glass bead medium, *Water Resour. Res.*, *4*(4), 809–815, 1968.

Kueper, B. H., and E. O. Frind, Two-phase flow in heterogeneous porous media, 1, Model development, *Water Resour. Res.*, *27*(6), 1049–1057, 1991a.

Kueper, B. H., and E. O. Frind, Two-phase flow in heterogeneous porous media, 2, Model application, *Water Resour. Res.*, *27*(6), 1059–1070, 1991b.

Lapidus, L., and N. R. Amundson, Mathematics of adsorption in beds: The effect of longitudinal diffusion in ion exchange and chromatographic columns, *J. Phys. Chem.*, *56*, 984–988, 1952.

Laryea, K. B., D. E. Elrick, and M. J. L. Robin, Hydrodynamic dispersion involving cationic absorption during unsaturated, transient water flow in soil, *Soil Sci. Soc. Am. J.*, *46*, 667–671, 1982.

Levenspiel, O., *Chemical Reaction Engineering*, 2nd Ed., John Wiley, New York, 1972.

Mansell, R. S., P. J. McKenna, and M. E. Hall, Simulated solute movement in wastewater-ponded soil, *Soil Sci. Soc. Am. J.*, *49*, 541–546, 1985.

Mansell, R. S., S. A. Bloom, B. Burgoa, P. Nkedi-Kizza, and J. S. Chen, Experimental and simulated P transport in soil using a multireaction model, *Soil Sci.*, *153*(3), 185–194, 1992.

Niibori, Y., and T. Chida, A model of local distribution of saturation in a fractured layer, and its application, paper presented at Nineteenth Annual Workshop on Geothermal Reservoir Engineering, Stanford Univ., Stanford, Calif., Jan. 18–20, 1994.

Niibori, Y., A. Kounosu, and T. Chida, Fundamental study on tracer response analysis for water-steam flow accompanied by boiling in a porous medium, *J. Geothermal Res. Soc. Jpn.*, *14*(2), 129–144, 1992.

Powers, S. E., C. O. Loureiro, L. M. Abriola, and W. J. Weber Jr., Theoretical study of the significance of nonequilibrium dissolution of nonaqueous phase liquids in subsurface systems, *Water Resour. Res.*, *27*(4), 463–477, 1991.

Powers, S. E., L. M. Abriola, and W. J. Weber Jr., An experimental investigation of nonaqueous phase liquid dissolution in saturated subsurface systems: Steady state mass transfer rates, *Water Resour. Res.*, *28*(10), 2691–2705, 1992.

Smiles, D. E., and B. N. Gardiner, Hydrodynamic dispersion during unsteady, unsaturated water flow in a clay soil, *Soil Sci. Soc. Am. J.*, *46*, 9–14, 1982.

Smiles, D. E., J. R. Philip, J. H. Knight, and D. E. Elrick, Hydrody-

namic dispersion during absorption of water by soil, *Soil Sci. Soc. Am. J.*, *42*, 229–234, 1978.

Smiles, D. E., K. M. Perroux, S. J. Zegelin, and P. A. C. Raats, Hydrodynamic dispersion during constant-rate absorption of water by soil, *Soil Sci. Soc. Am. J.*, *45*, 453–458, 1981.

Smiles, D. E., W. R. Gardner, and R. K. Schulz, Diffusion of tritium in arid disposal sites, *Water Resour. Res.*, *31*(6), 1483–1488, 1995.

Unger, A. J. A., E. A. Sudicky, and P. A. Forsyth, Mechanisms controlling vacuuming extraction coupled with air sparging for remediation of heterogeneous formations contaminated by dense nonaqueous phase liquids, *Water Resour. Res.*, *31*(8), 1913–1925, 1995.

Wehner, J. F., and R. H. Wilhelm, Boundary conditions of flow reactor, *Chem. Eng. Sci.*, *6*, 89–93, 1956.

White, I., D. E. Smiles, and K. M. Perroux, Absorption of water by soil: The constant flux boundary condition, *Soil Sci. Soc. Am. J.*, *43*, 659–664, 1979.

Wilson, D. J., *Modeling of In Situ Techniques for Treatment of Contaminated Soils*, Technomic, Lancaster, U. K., 1995.

Wilson, J. L., and L. W. Gelhar, Analysis of longitudinal dispersion in unsaturated flow, 1, The analytical method, *Water Resour. Res.*, *17*(1), 122–130, 1981.

Yule, D. F., and W. R. Gardner, Longitudinal and transverse dispersion coefficients in unsaturated plainfield sand, *Water Resour. Res.*, *14*, 582–588, 1978.

T. Chida and D. Haga, Department of Geoscience and Technology, Graduate School of Engineering, Tohoku University, Sendai 980-8579, Japan. (haga@gogh.earth.tohoku.ac.jp)

Y. Niibori, Department of Quantum Science and Energy Engineering, Graduate School of Engineering, Tohoku University, Sendai 980-8579, Japan.

(Received October 13, 1998; revised November 30, 1998; accepted December 4, 1998.)